Electronic Supplementary Material (ESI) for Polymer Chemistry.

Supporting Information

Polymer brush-assisted microcontact printing: Using tailor-made polydimethylsiloxane (PDMS) stamp for precise patterning of rough surfaces

*Nazim Pallab,[ab] Stefan Reinicke,[b] Johannes Gurke,[ab] Rainer Rihm,[b] Sergio Kogikoski Jr.,[a] Matthias Hartlieb,[ab] and Martin Reifarth[ab]**

[a]Chair of Polymer materials and Polymer Technologies, University of Potsdam

Karl- Liebknecht- Straße 24-25, 14476 Potsdam, Germany

[b]Fraunhofer Institute for Applied Polymer Research

Geiselbergstraße 69, 14476 Potsdam, Germany

** To whom correspondence should be addressed:*

martin.reifarth@uni-potsdam.de

N-acryloxysuccinimide (NAS) synthesis:

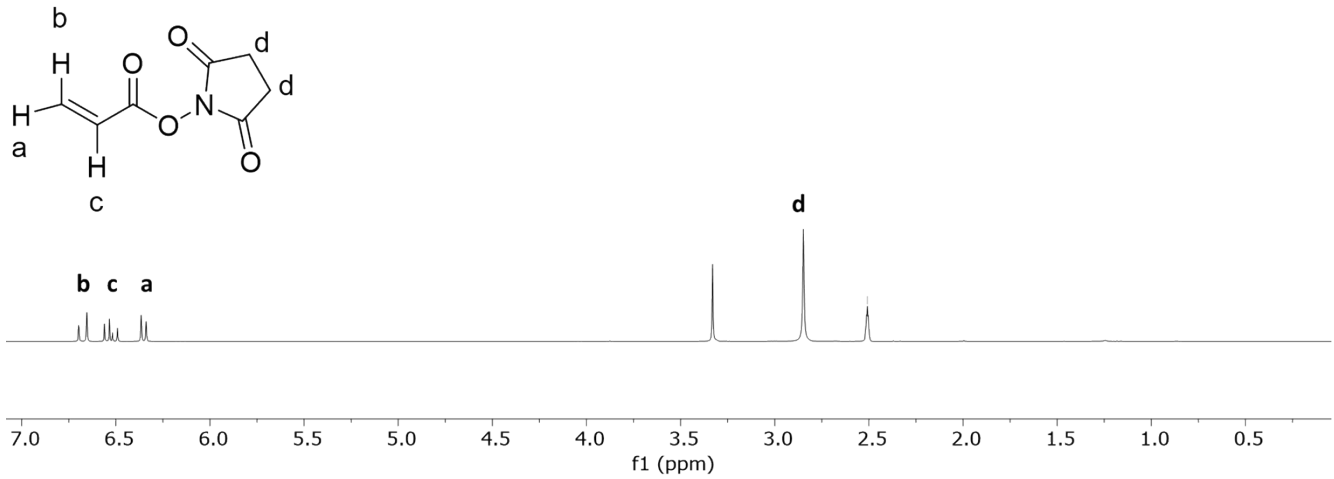

Figure S1. ^{1}H NMR Spectra of *N*-acryloxysuccinimide (Solvent used was DMSO-(d_6) and the spectra were analyzed with MestreNova 12.0).

^{1}H NMR (400 MHz, DMSO-d_6): 6.68 (dd, C*H*, 1H), 6.53 (dd, C*H,* 1H), 6.35 (dd, C*H,* 1H), 2.85 (s, COC*H,* 4H).

Poly(80%butyl acrylate-*co*-20%N-acryloxysuccinimide) Crosslinker Synthesis:

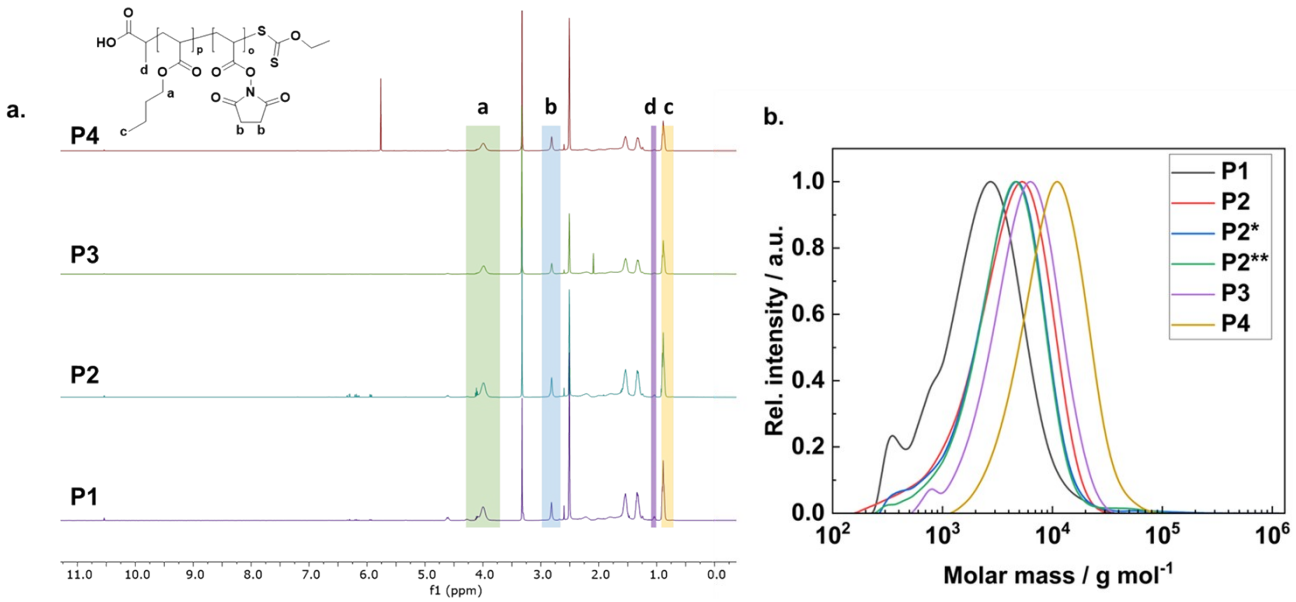

Figure S2. a) ^{1}H NMR Spectra of poly(80%BA-*co*-20%NAS) of different targeted degree of polymerization (DP). Dichloromethane (DCM) peak at 5.3 ppm of top spectra (DP ~ 50) comes from the solvent used for dissolving the polymer for easy handling. **b)** SEC profiles of poly(80%BA-*co*-20%NAS) (THF as an eluent, PS-calibration). Characterization data are listed in the following **Table S1**.

Table S1. Characterization data, *i.e.* degree of polymerization, molar mass (M_n), dispersity (Đ), of crosslinker copolymers. SEC was performed in THF, using polystyrene (PS)-standards.

Crosslinker	Targeted DP	Targeted M_n (g mol^{-1})	Measured M_n ^{1}H-NMR	Measured Mn, SEC (g mol^{-1})	Đ
P1	10	1362	1403	1490	2.10
P2	20	2724	2893	2583	2.05
P2*	20	2724	2980	2646	2.02
P2**	20	2724	3021	2827	1.87
P3	30	4086	3144	3318	1.26
P4	50	6810	6851	8072	1.56

*/** These batches of polymer were used for mechanical characterization and further printing experiments.

Stamp preparation:

Stamp	NAS-to-APMS ratio	Crosslinker's DP	Curing temperature	Crosslinking efficiency
St1	0.25	10	90 °C	Poor
St2	0.3	10	90 °C	Poor
St3	0.5	10	90 °C	Optimum
St4	0.5	20	90 °C	Optimum
St5	0.5	20	110 °C	Optimum
St6	0.5	30	90 °C	Optimum
St7	0.75	10	90 °C	Optimum
St8	0.8	50	90 °C	Not optimized*
St9	1	10	90 °C	Optimum
St10	1	20	90 °C	Optimum
St11	1	20	110 °C	Optimum
St12	1	30	90 °C	Optimum
St13	1.4	20	90 °C	Poor
St14	1.4	30	90 °C	Poor
St15	1.6	30	90 °C	poor

Table S2. Stamp preparation with different crosslinkers with varying NAS-to-amino ratios.

*Stamp prepared with DP ~ 50 crosslinker was not optimized because of the waxy behavior of the polymer and appeared unfavorable for smooth mixing with 6-7%APMS-*co*-DMS prepolymer. Amino functionality of 6-7%APMS-*co*-DMS upon mixing with the crosslinker had undergone rapid crosslinking.

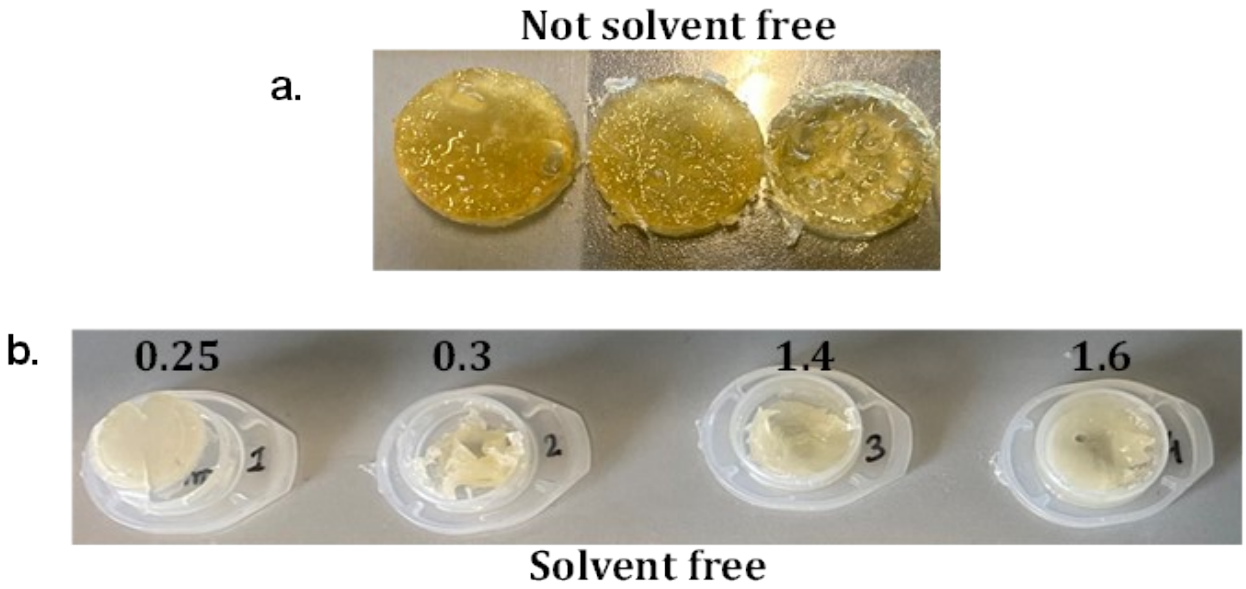

Figure S3. Incomplete crosslinking of prepared stamp. **a**) Incomplete crosslinking seen when solvent used to dissolve poly(80%BA-*co*-20%NAS) crosslinker. **b)** Inefficient crosslinking observed during stamp preparation with different ratio of NAS-to-APMS (**St1**, **St2**, **St13**, and **St15** from left to right).

In **Figure S3a** poorly crosslinked stamps are shown. Stock solution of the crosslinker was prepared in ethyl acetate to accommodate flexible handling and mixing of the crosslinker to the prepolymer at different mixing ratios of (NAS-to-APMS). The crosslinking was poor due to incomplete solvent evaporation during curing at different temperatures (90 ° & 110 °C). **Figure S3b** shows that poor crosslinking depends on the mixing ratio of NAS-to-APMS as well. Stamps cured in a solvent free environment still demonstrated poor crosslinking at a ratio of NAS-to-APMS < 0.5 and > 1.

Microcontact Printer:

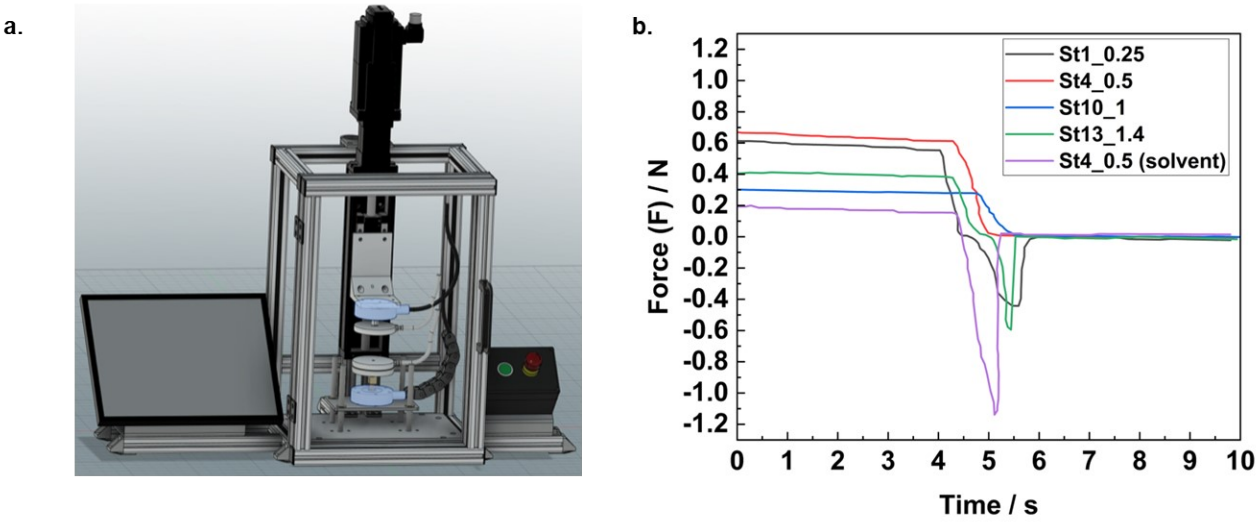

Figure S4. a) Representation of the ZumoLab Microcontact Printer (Zumo-MCP) depicting force sensors positioned above and below the upper and lower plates (in blue) respectively. The attached computer also monitors different parameters, such as pressure, ramp-up and -down rates, etc. via Zumo-MCP software. **b)** Stickiness measurement of the stamps (**St1, St4, St10, St13,** & **St4 with solvent presence** within the preparation procedure). Retraction force was measured with the help of "Zumo-MCP". A set force 0.5 N was applied for 3s (samples fixed and sandwiched between two plates) with a ramp up rate of 0.05 N s^{-1}. The retraction force during withdrawal of the upper plate was measured. The sticky samples show higher retraction force during the withdrawal of the upper plate.

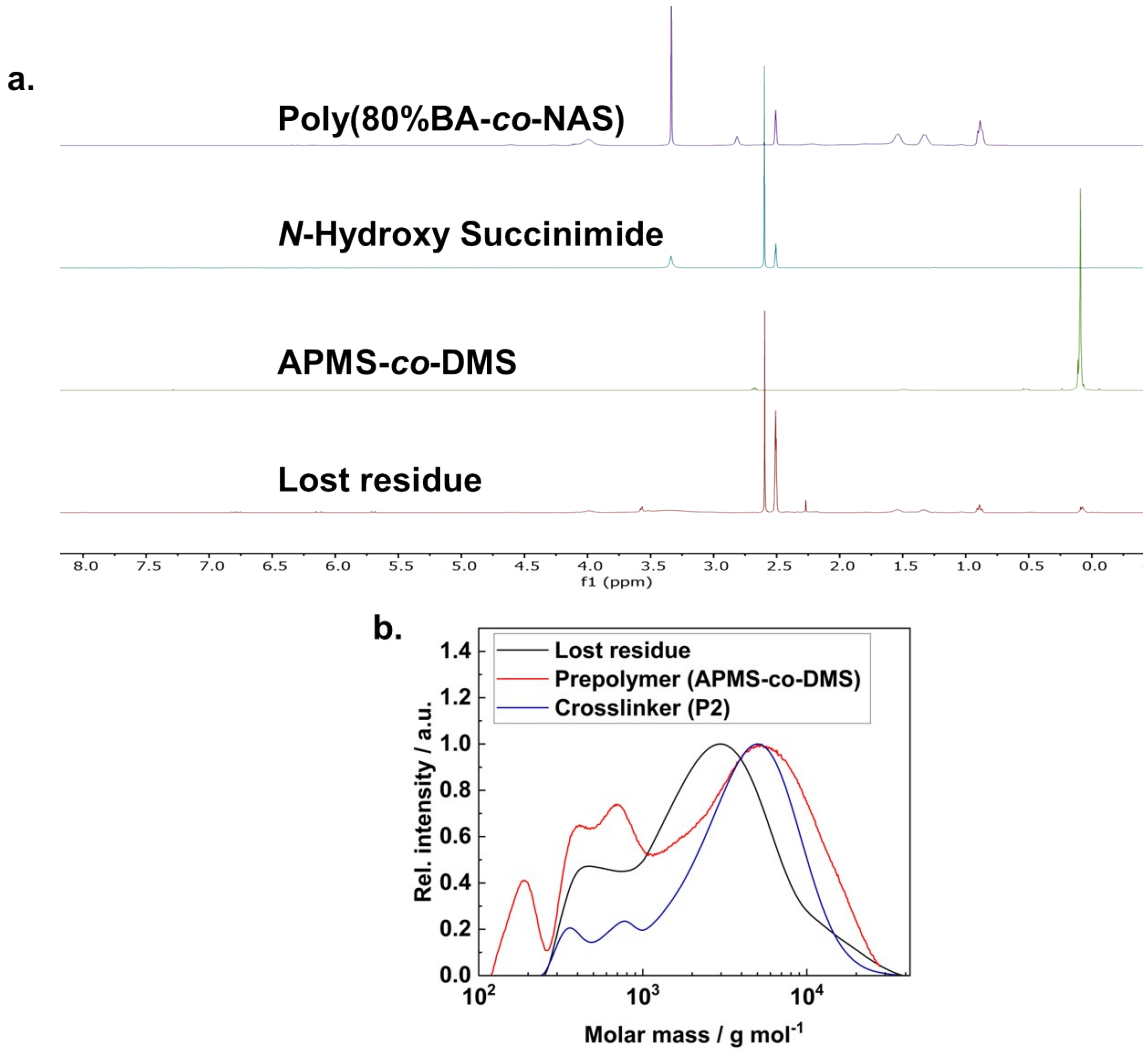

Figure S5. Characterization of lost residue of swollen stamp **(St4)**. a) ^{1}H NMR spectra of lost residue and comparison with corresponding contents used during stamp production (measured in DMSO, d_6, 2.50 ppm). b) SEC profiles of lost residue and comparison with the raw materials for stamp production (PS calibration, THF as eluent).

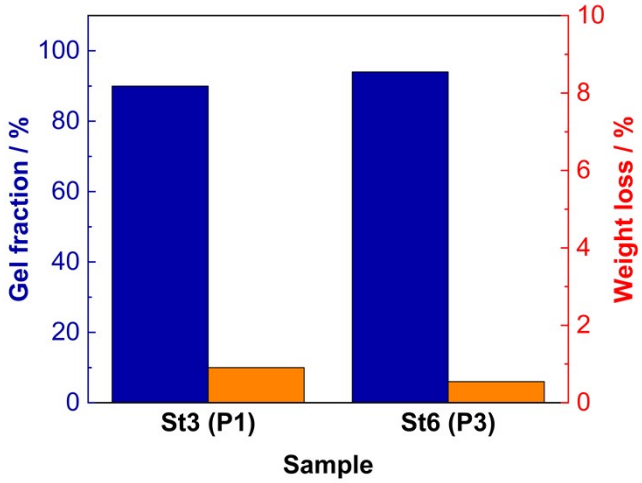

Figure S6. Gel fraction (%) and weight loss (%) of **St3** (**P1**) and **St6** (**P3**). More weight loss was seen for **St3** where crosslinker with a low DP was used.

Mechanical Properties:

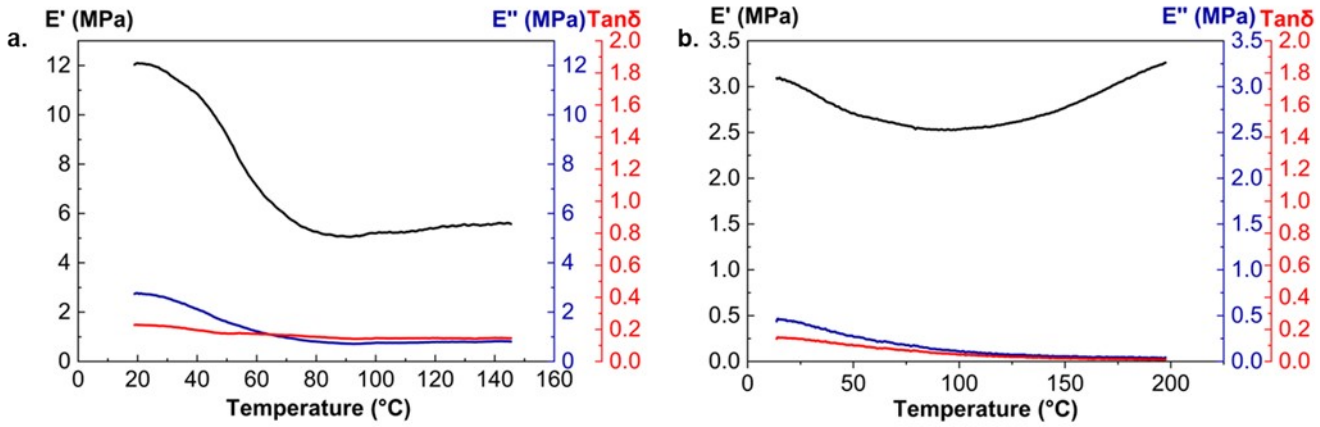

Figure S7. DMA analyses of PDMS stamps (**CSt1**, cured at 110 °C) conducted at 10 Hz and 5K min^{-1}. **a)** Compression profile of PDMS (F_{dyn} ~ 2N, sample size ~ 0.9 cm^2). **b)** Tension profile performed at 10 Hz and with 5K min^{-1} temperature ramp.

Figure S7a illustrates the response of conventional PDMS stamp (**CSt1**) when subjected to a compressive dynamic force ranging around 2 N at temperatures between 20°C and 150°C. At room temperature, **CSt1** exhibits a storage modulus (E') of approximately 12 MPa. This modulus decreases as temperature rises, eventually reaching a plateau at approximately 90°C, resembling the compression behavior observed in the novel stamp (**St5**) showcased in **Figure 4a**. Similarly, **Figure S7b** demonstrates that the tension profile of PDMS also exhibits elastomeric characteristics analogous to the tension profile observed in **Figure 4b** for the novel stamp. In both cases, there is a higher elastic component (E') and lower viscous components (E''), indicated by a phase mismatch represented by tan δ. The increase in temperature results in an upward surge in the storage modulus (E'), signifying robust crosslinking within the network. Specifically, the storage modulus of **CSt1** material at room temperature is measured at approximately 3.1 MPa.

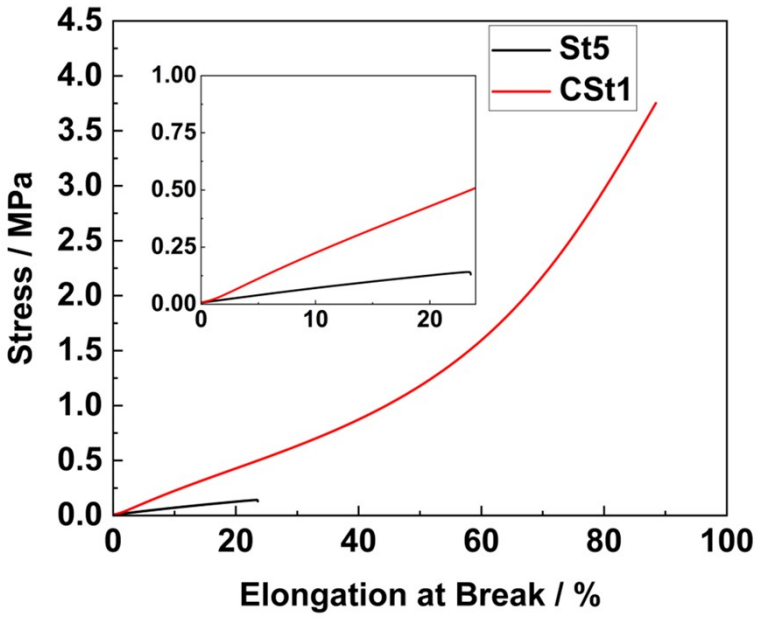

Figure S8. Quasi-static uniaxial tensile test of novel stamp material (**St5**) and PDMS (**CSt1**) in comparison. Young's modulus is recorded from the slope of stress-strain curve at 2.68 ± 0.1 MPa and 0.68 ± 0.4 MPa, respectively. The ultimate tensile strength and elongation at break (%) are recorded at 3.86 ± 0.5 MPa and 88 ± 6% for **CSt1** respectively. A comparatively lower elongation at break (%) and ultimate tensile strength are recorded for **St5** (24.1 ± 0.4% and 0.14 ± 0.01 MPa respectively). Note that within the elongation limit of **St5**, **CSt1** demonstrates a similar behavior shown in the inset.

Table S3: Characterization data (targeted degree of polymerization, molar mass (M_n), dispersity indices (Đ) of grafted PTrisAAm polymer from the stamps with different NHS-acrylate-to-amino (NAS-to-APMS) ratios.

Grafted polymer	Targeted DP	Targeted M_n (g mol^{-1})	NAS-to-APMS	Stamp & curingtemp.	M_n[a] (g mol^{-1})	Đ
GP1	200	35,000	0.5	St4, 90 °C	14,334	1.69
GP2	1000	175,000	0.5	St5, 110 °C	26,953	4.13
GP3	1000	175,000	1	St5, 110 °C	40,000	3.10
GP4	1500	262,500	0.5	St5, 110 °C	43,025	3.15
GP5	800	140,000	0.5	St4, 90 °C	41,970	2.66
GP6*	1000	175,000	0.5	St4, 90 °C	46,000	4.60
GP7	1000	175,000	0.5	St4, 90 °C	81,000	2.99

[a]Measured by SEC (PVP calibration, using aqueous solution with 0.3 vol% formic acid, and 0.1M NaCl as SEC eluent). (*) GP6: Poly(*N*-acryloyl morpholine) acryl amide as grafted polymer.

Surface Functionalization, Patterning & Printing:

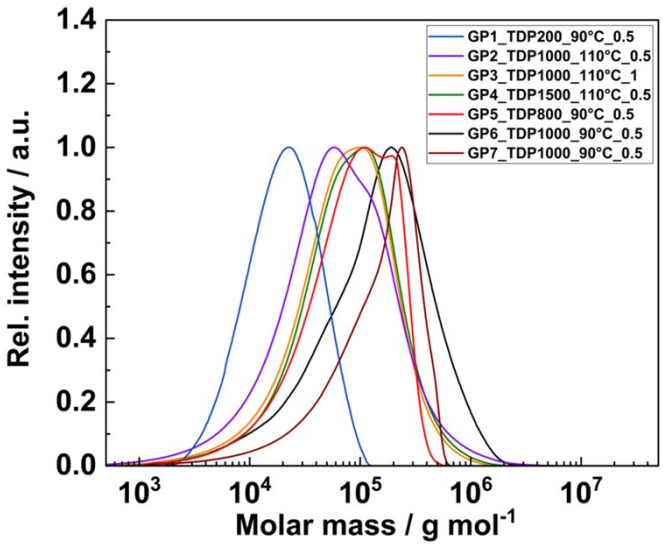

Figure S9. SEC profiles of grafted polymers in the solution (stamps, **St4&5** cured at 90 °C & 110 °C respectively, shuttle CTA approach). Along with targeted degree of polymerization (TDP), NAS-to-APMS ratio of grfated stamps are also mentioned in the legend section. Aqueous solution with 0.3 vol% formic acid, and 0.1M NaCl was used as SEC eluent (PVP-calibration).

Inking of PTrisAAM Polymer in Solution:

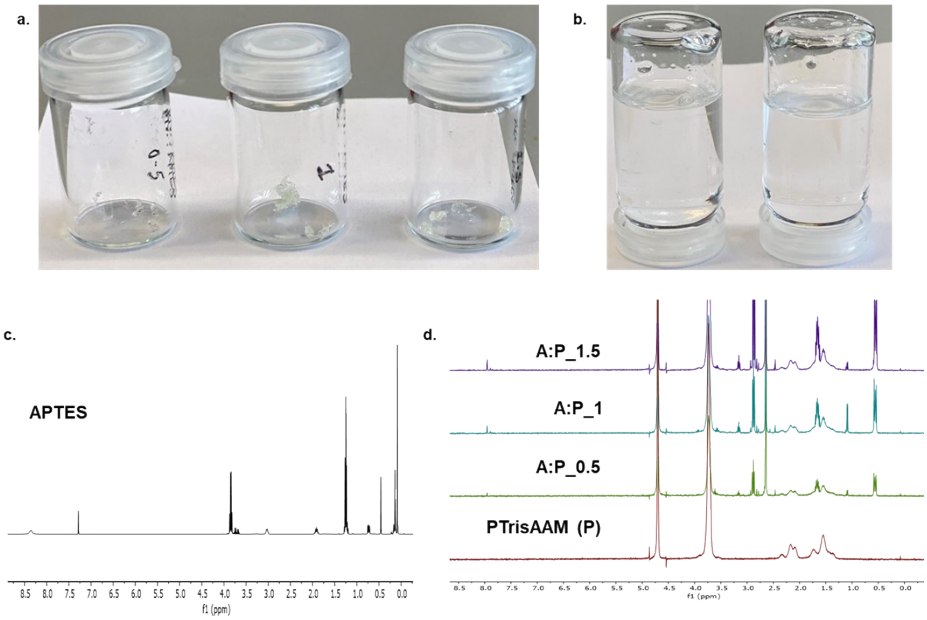

Figure S10. a) APTES-PTrisAAM- (**A:P**) conjugates in different molar ratios (0.5, 1, & 1.5 respectively from left to right). APTES was combined with PTrisAAm polymer in dry DMF at 100 °C for 3h in presence of sodium hydroxide catalyst. **b)** Crosslinked products (1 (left) & 1.5 (right) shown) showed poor solubility in solvent (DMSO). **c)** ^{1}H NMR spectra of APTES in $CDCl_3$ (7.26 ppm). NMR tube was plasma treated and passivated with chlorotrimethylsilane prior to analysis. Peak at ~ 0 ppm is from chlorotrimethylsilane. -Si***C***H_2 peak is recorded at 0.8 ppm. **d)** ^{1}H NMR spectra of PTrisAAm polymer and APTES-PTrisAAM (**A:P**) conjugates in D_2O (4.7 ppm). The presence of -Si***C***H_2 peak along with polymeric backbones between 1.2 – 2.5 ppm shows the polymer-APTES conjugate formation. Partial hydrolysis of APTES is suggested by the emergence of sharp peaks instead of broad peaks at ~1.6 ppm and 0.6 ppm.

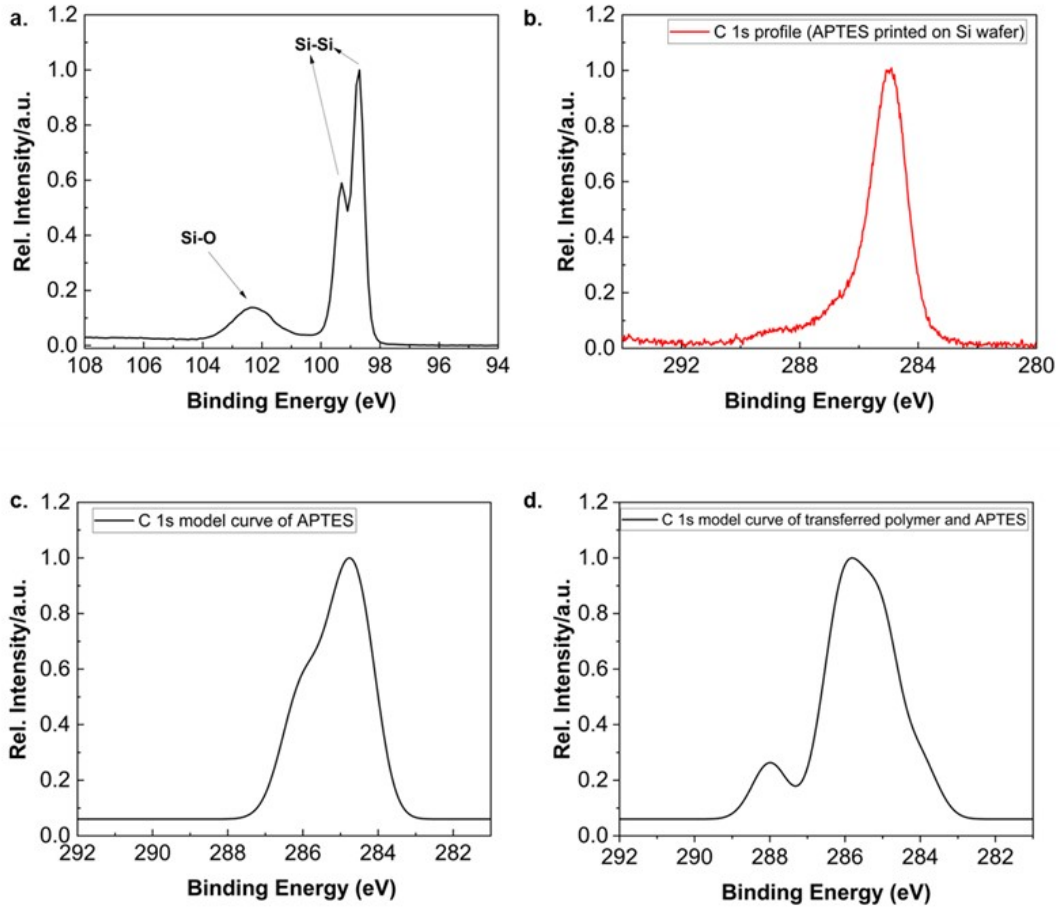

Figure S11. a) Si (2p) spectra of a plasma-treated bare Si wafer substrate. **b)** C (1s) XPS spectra of APTES-printed Si wafer corresponding to the printing experiment with novel stamp (**St4**). **c)** A simulated C (1s) profile of printed area containing only APTES. **d)** A simulatedl C (1s) profile of printed area containing polymer content and APTES together.

The presence of APTES transfer is corroborated by observing the C (1s) spectra within the range of 288 eV to 290 eV in Figure S8b, coupled with the N (1s) spectra in **Figure 6b**. A comparison between the model curves (**Figure S11c& d**) and the experimental data in **Figure S11b** confirms that the areas beneath the curves, specifically the characteristic peaks of C-C and C-N, signify the presence of APTES transfer. Moreover, a subtle peak around ~288 eV (**Figure S11b**) corresponds to the carbonyl group (C=O). This particular carbonyl group is attributed to the transferred grafted PTrisAAm polymer brush as well as the carbonyl content originating from the stamp during the printing process.

Inking and Ink Transfer Mechanism:

The covalent attachment of the ink (APTES) to the surface grafted PTrisAAm polymer occurs in solution. APTES is a reactive silane with three ethoxy groups and an amine group in its structure, and PTrisAAm offers hydroxy functional groups in his monomeric unit. The binding of APTES to an oxidic initiates *via* hydrolytic cleavage of triethoxy moieties present in APTES by forming silanol and releasing ethanol. The silanol groups form siloxane (Si-O-Si) bridges *via* condensation in horizontal or vertical orientation along the surface. The condensation of silanol can also result in branched structure due to network formation and hydrogen bond formation between the primary amine group of silane and the oxide surface.[1,2] Accordingly, oligomolecular APTES layers form at the substrate surface.

When APTES is exposed to the PTrisAAm polymer, applying elevated temperatures and under NaOH catalysis, APTES will attach in a covalent fashion to the polymer. Ideally, APTES molecule would bind to the existing hydroxy groups of the monomeric unit of PTrisAAm to form a cage like structure such as silatranes. This formation Polymer-APTES conjugation is complex and was discussed in our previous work.[3]

Due to alkoxysilane's tendency to undergo hydrolysis, water content and pH can influence the formation of silanol. It has been reported that the acidic pH initiate hydrolysis of APTES, whereby basic pH can contribute to both hydrolyse and condensation. [1,4] For printing, the ink-attached stamp is exposed to chemical vapor deposition (CVD) of acetic acid and water in a close container to initiate hydrolysis. Therefore, the acidic pH and water content influence faster silanol formation on the stamp surface.[4] Self-polymerization or condensation of silanol to siloxane bridge formation would occur once the stamp comes in contact with the activated oxide surface. In solution, a period of 20-60 min was sufficient for APTES deposition,[5,6] where times as less as 10 min was used in vapor phase[7] in different studies. In our study, a prolonged contact of 20 min was maintained for μCP. Note that a deeper analysis of the printing mechanism would be required, which will be the scope of a follow-up study.

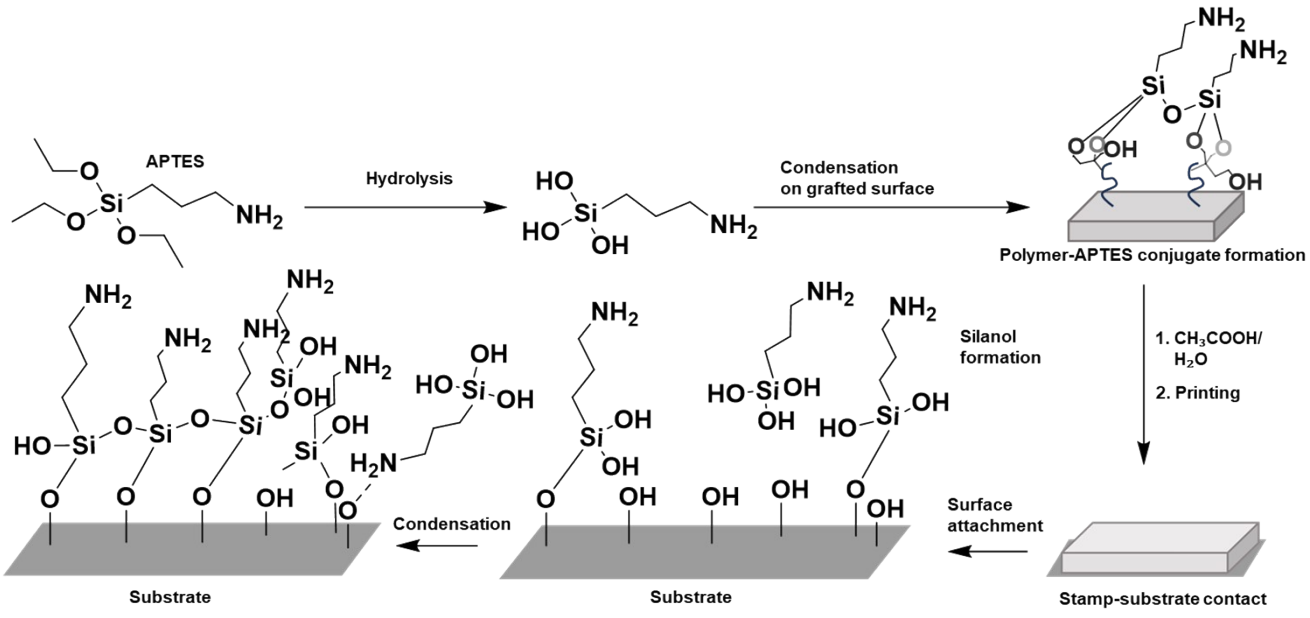

Scheme S1. Illustration of possible routes for APTES transfer mechanism. APTES transfer mainly occurs in 2 steps: a) hydrolysis and 2) condensation. Initially APTES forms silanol and then ideally forms APTES-polymer conjugate. The stamp is exposed to acidic pH (acetic acid CVD) and moisture (water content) prior to printing. During µCP stable siloxane bridge forms with plasma treated oxide substrate *via* condensation.

Patterned Surface:

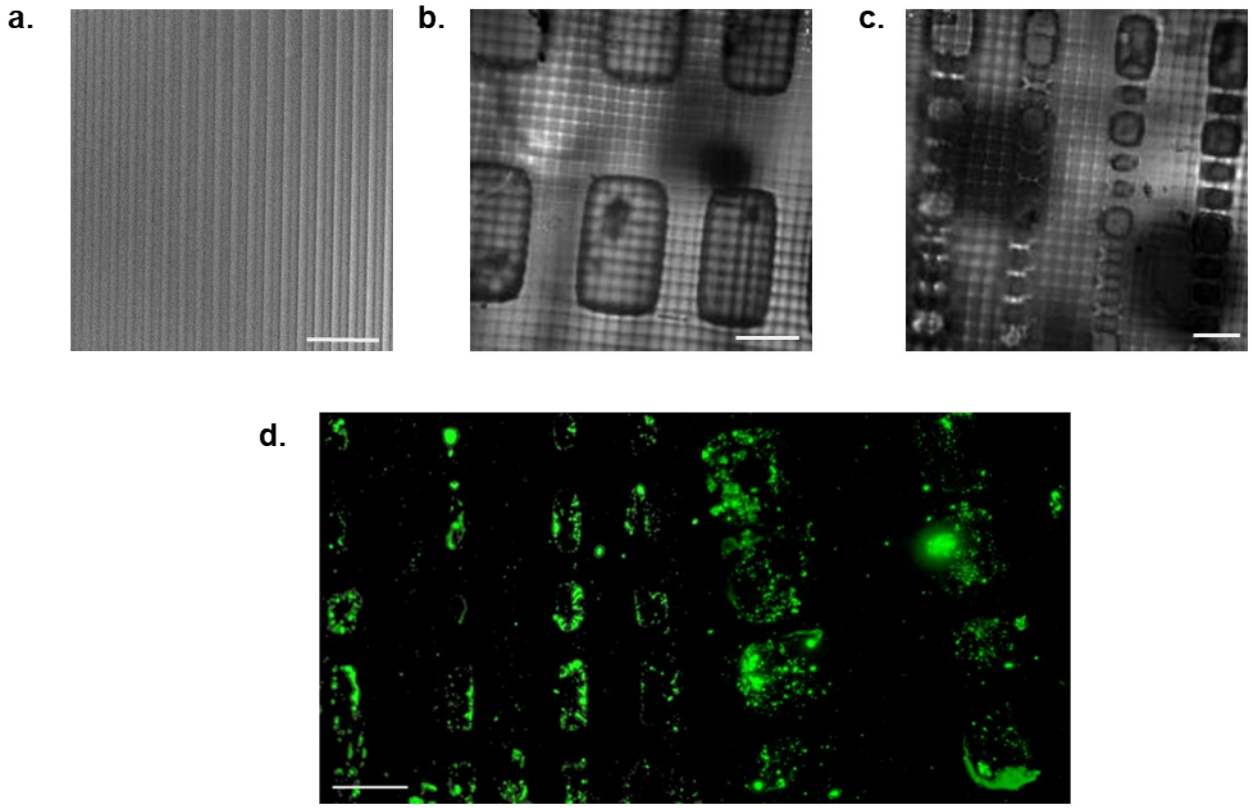

Figure S12. a) Light microscope image of patterned stamp (4 µm stripes patterned with a Si master, 20x magnification)**. b & c)** Light transmission micrographs of patterned stamp surface with a custom-designed 3D mold as the master template. **d)** Fluorescence micrograph of transferred patterns onto smooth Si wafer surface. The images are stitched, gamma (0.38) and brightness corrected on imageJ. The scale bars are 20 µm.

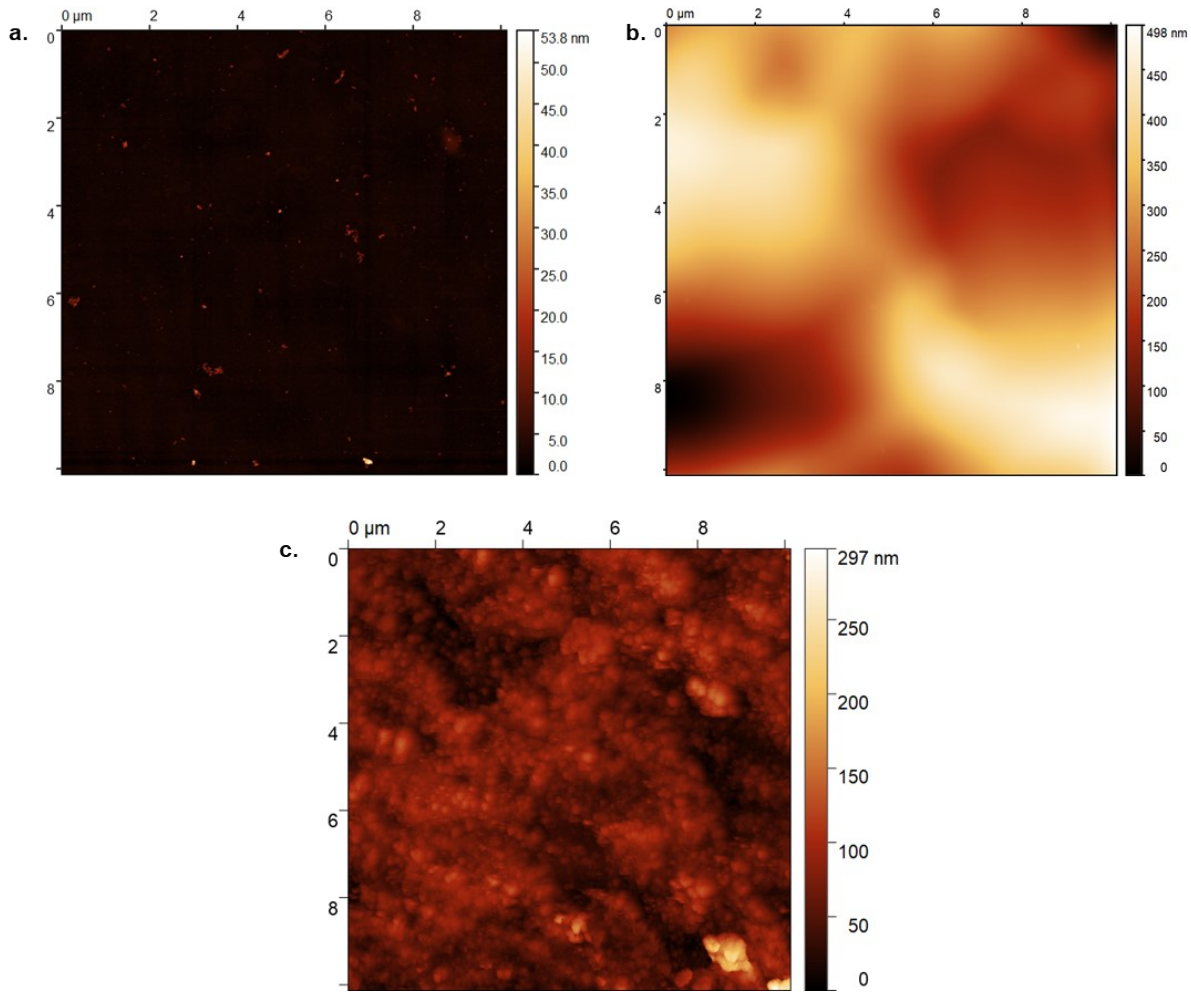

Figure S13. Atomic force microscopy (AFM) height images. **a**) Smooth side of pristine Si wafer. **b)** Rough side of pristine Si wafer. **c)** Silica-gel modified glass substrate. Data leveling by mean plane subtraction of the images were performed on Gwyddion. Roughness value are measured from statistical parameters of Gwyddion, average roughness value, R_a were measured at ~ 0.69 nm, ~ 105 nm, and ~ 93 nm for silica-gel modified glass, smooth side of Si wafer, and rough Si wafer respectively. The images are 10 × 10 µm.

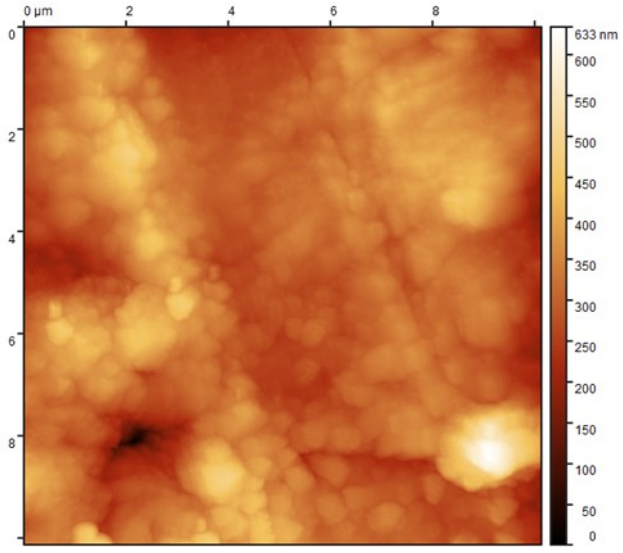

Figure S14. Atomic force microscopy (AFM) height image of 3D mould (master template). Data leveling by mean plane subtraction of the image was performed on Gwyddion. Roughness value was measured from statistical parameters of Gwyddion, average roughness value, R_a were measured at ~ 69 nm. The image is 10 × 10 µm.

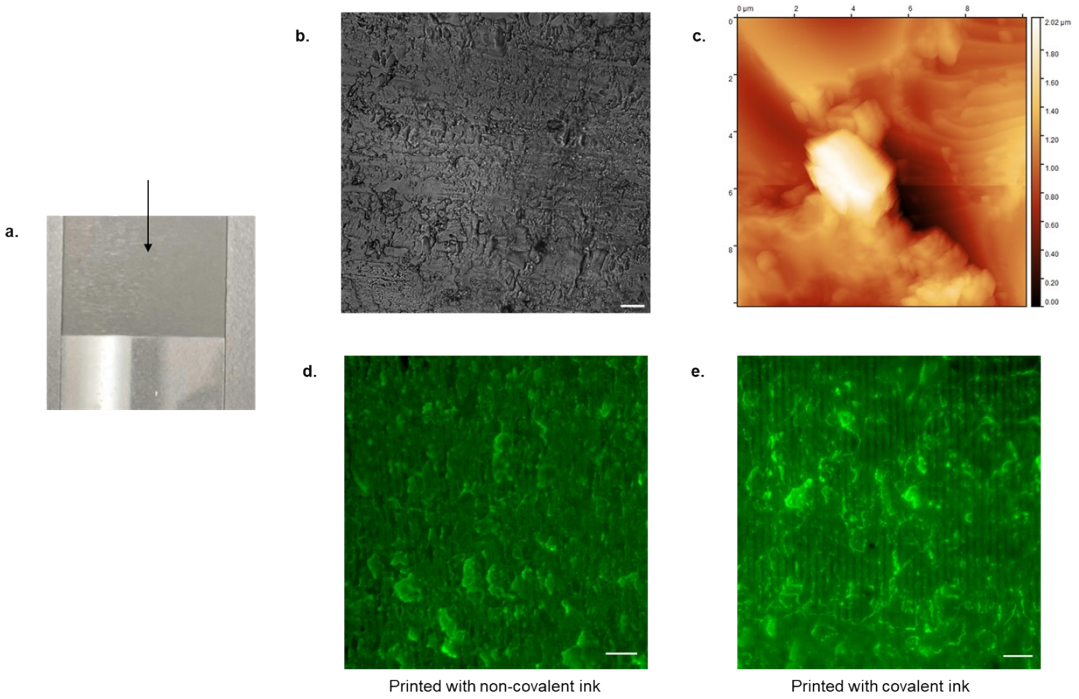

Figure S15. a) Photography of a rough glass substrate, which is a sandblasted part of a glass slide. **b)** Light microscopy image of the rough glass. **c)** Atomic force microscopy (AFM) height image of the rough glass surface. Data leveling by mean plane subtraction and polynomial background subtraction of the image were performed on Gwyddion. Roughness value was measured from statistical parameters of Gwyddion, average roughness value, R_a were measured at ~ 314 nm. The image is 10 × 10 µm. **d)** Fluorescence image of 4 µm stripe patterns printed on rough glass surface. Ink (APTES) was drop-casted to attach it to the grafted polymer surface non-covalently. The inked-stamp was used for printing. **e)** Fluorescence image of 4 µm stripe patterns printed on rough glass surface. Ink (APTES) was reacted with grafted polymer for 3h at 60 °C in MeOH to attach it to the grafted polymer surface covalently. The inked-stamp was used for printing afterward. Covalently-grfated ink has more precisely been transferred to the rough glass surface compared to the non-covalently attached counterpart. The scale bars are 20 µm.

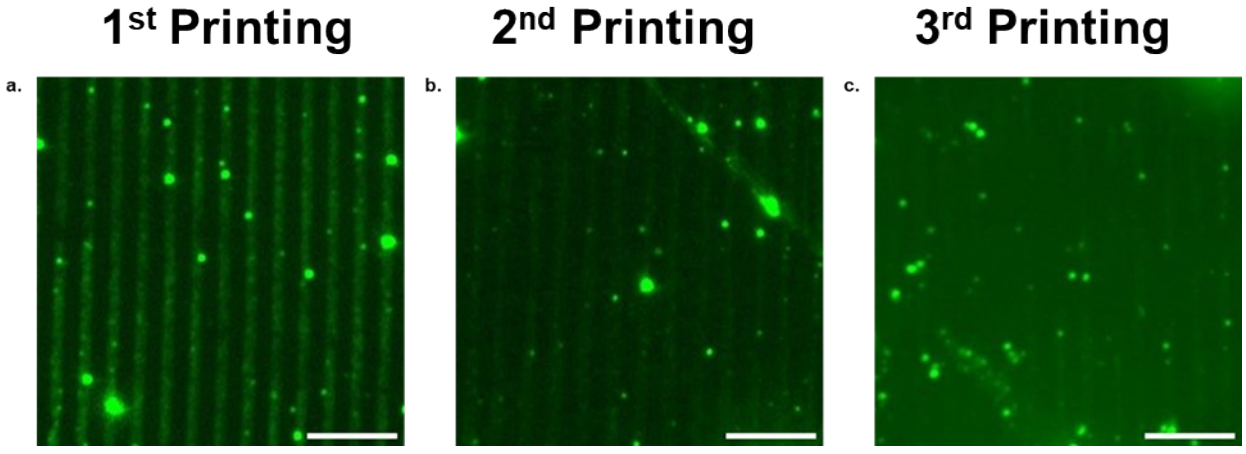

Figure S16. Fluorescence microscope images of 4 µm stripe patterns printed 3 times consecutively to evaluate printing efficiency. **a**) First printing shows sharp patterns **b)** Second consecutive printing shows gradual ink fading. **c)** Third printing shows almost faded structures under the microscope. The images are stitched, gamma (0.38) and brightness corrected on imageJ. The scale bars are 20 µm.

References:

[1] M. Sypabekova, A. Hagemann, D. Rho, S. Kim, Biosensors 2022, **13**, 36.
[2] Y. Liu, Y. Li, X.-M. Li, T. He, Langmuir 2013, **29**, 15275.
[3] P. Akarsu, R. Grobe, J. Nowaczyk, M. Hartlieb, S. Reinicke, A. Böker, M. Sperling, M. Reifarth, ACS Appl. Polym. Mater. 2021, **3**, 2420.
[4] M.-C. Brochier Salon, P.-A. Bayle, M. Abdelmouleh, S. Boufi, M. N. Belgacem, Coll. Surf. A: Physicochem. Eng. Asp. 2008, **312**, 83.
[5] A. Miranda, L. Martínez, P. A. A. De Beule, MethodsX 2020, **7,** 100931.
[6] M. Antoniou, D. Tsounidi, P. S. Petrou, K. G. Beltsios, S. E. Kakabakos, Med. Devices Sens. 2020, **3**, e10072.
[7] Y. Liang, J. Huang, P. Zang, J. Kim, W. Hu, Appl. Surf. Sci. 2014, **322**, 202.